

Self-phase modulation of a single-cycle terahertz pulse by nonlinear free-carrier response in a semiconductor

Dmitry Turchinovich,^{1,2,*} Jørn M. Hvam,¹ and Matthias C. Hoffmann³

¹*DTU Fotonik, Technical University of Denmark, DK-2800 Kgs. Lyngby, Denmark*

²*Max Planck Institute for Polymer Research, Ackermannweg 10, 55128 Mainz, Germany*

³*SLAC Linear Accelerator Laboratory, 2575 Sand Hill Road, Menlo Park, California, 94025, USA*

(Received 23 January 2012; published 29 May 2012)

We investigate the self-phase modulation (SPM) of a single-cycle terahertz pulse in a semiconductor, using bulk *n*-GaAs as a model system. The SPM arises from the heating of free electrons in the electric field of the terahertz pulse, leading to an ultrafast reduction of the plasma frequency, and hence to a strong modification of the terahertz-range dielectric function of the material. Terahertz SPM is observed directly in the time domain. In the frequency domain it corresponds to a strong frequency-dependent refractive index nonlinearity of *n*-GaAs, found to be both positive and negative within the broad spectrum of the terahertz pulse, with the zero-nonlinearity point defined by the electron momentum relaxation rate. We also observed the nonlinear spectral broadening and compression of the terahertz pulse.

DOI: [10.1103/PhysRevB.85.201304](https://doi.org/10.1103/PhysRevB.85.201304)

PACS number(s): 78.20.-e, 42.65.Re, 72.20.Ht, 78.47.J-

Since its first demonstration¹ more than five decades ago, nonlinear optics (NLO) has revolutionized the field of photonics. Until recently, ultrafast NLO was largely confined to the visible and infrared spectral ranges. However, with the emergence of sources generating high-energy ultrafast single-cycle terahertz (THz) pulses,^{2–4} more and more NLO studies are being conducted in the THz range. Nonlinear dynamics in semiconductors in strong THz fields is a particularly rich area of research due to good coupling between the THz fields and free carriers, and due to the possibility of inducing strong polarization effects in semiconductors with strong THz signals.⁵ Many interesting ultrafast phenomena have been investigated recently, such as interaction of strong THz fields with excitons,^{6,7} THz-induced impact ionization of electrons in narrow-gap semiconductors,^{8,9} ultrafast THz-induced electron dynamics in complex conduction bands,^{10–14} and femtosecond all-optical switching in nanoscale structures with THz signals.^{15,16}

The majority of studies in the present-day ultrafast THz NLO are focused on achieving a better understanding and control of nonlinear processes in (mostly semiconductor) materials using THz light. There are, however, very few reports aiming at control and manipulation of THz light making use of the material's nonlinear response. Yet, the ultrafast THz signals are usually single-cycle wave forms, which can be experimentally sampled with a time resolution much better than one optical cycle, providing the complete time-domain information about the optical signal—its amplitude and phase.^{17,18} As we will show in this Rapid Communication, this makes the THz pulses ideal tools for the direct observation of both (i) the THz-specific NLO phenomena and (ii) the general NLO phenomena occurring in the single-cycle optical regime.

Single-cycle pulses can not be described by the traditional carrier-envelope approximation.¹⁹ Irrespective of the frequency range to which they belong, they inherently have an extremely broad spectral bandwidth covering many octaves of frequencies. Hence the propagation of such signals in the medium is governed by the complex-valued material dielectric function $\hat{\epsilon}(\omega)$ covering a very broad spectral range.

An optical nonlinearity—the near-instantaneous modification of this dielectric function due to a nonlinear light-matter interaction occurring in the single-cycle regime, corresponds to a modification of the optical properties of matter over an extremely broad range of frequencies. We find the effect of such a sudden change of dielectric environment on the propagating single-cycle wave form to be quite intriguing, which is the motivation behind the present work.

In this Rapid Communication, we report on the study of a fundamental nonlinear optical effect—the self phase modulation (SPM)^{20,21} of a single-cycle THz pulse. The SPM occurs due to the change of the (real part of) refractive index $n(\omega) = \text{Re} \sqrt{\hat{\epsilon}(\omega)}$ of the material as a result of light-matter interaction. As an efficient nonlinear medium for the THz range we used an *n*-doped bulk semiconductor GaAs, whose optical nonlinearity arises from the response of free electrons to the THz fields. We note that any other doped or photoexcited semiconductor with a complex band structure will also exhibit the THz-range SPM according to the mechanism described here. The SPM was observed by us directly in the time domain using THz time-domain spectroscopy (TDS)^{17,18} and was analyzed in the frequency domain.

In this Rapid Communication, we show that the THz-range optical nonlinearity of a doped or photoexcited semiconductor is based on the modification of its plasma frequency by the carrier heating in the THz field. Semiconductors with free carriers are good absorbers of THz radiation, and their THz-range complex-valued dielectric function $\hat{\epsilon}(\omega)$ is well described by the basic Drude plasma model^{22,23}

$$\hat{\epsilon}(\omega) = (n + i\alpha c/2\omega)^2 = \epsilon_{dc} - \omega_p^2/(\omega^2 - i\omega/\tau_r) \quad (1)$$

or by one of its extensions.^{24,25} Here, n and α are the frequency-dependent refractive index and power absorption coefficient, respectively, τ_r is a carrier momentum relaxation time, and ϵ_{dc} is the background “static” dielectric constant of the semiconductor in the absence of free carriers.²⁶ $\omega_p = (Ne^2/\epsilon_0 m)^{1/2}$ is the plasma frequency, where e is the elementary charge, N is the free-carrier density, ϵ_0 is the vacuum permittivity, and m is the carrier effective mass.

It directly follows from Eq. (1) that the change in plasma frequency ω_p resulting from the THz light-matter interaction will lead to a change in the THz absorption α and the refractive index n of the semiconductor, i.e., to nonlinear absorption and SPM. In the limiting case of $\omega_p \rightarrow 0$ the THz absorption will vanish, and the THz refractive index will be defined by the background dielectric constant $n(\omega_p \rightarrow 0) = \sqrt{\epsilon_{dc}}$. The only mechanism to reduce the plasma frequency in a doped semiconductor (i.e., where N is fixed) is the increase of the carrier effective mass m . In n -doped materials (e.g., n -GaAs), this can be achieved by electron heating in a sufficiently strong electric field by redistribution of the electron population in energy-momentum space of the conduction band from low-momentum, small-effective-mass states around the bottom of the Γ valley to high-momentum, large-effective mass states in the satellite valleys and to the states of strong nonparabolicity within the Γ valley (see, e.g., Ref. 27 and references therein). In p -doped materials, the hole scattering between the hole subbands can be utilized.

Recently, the carrier heating in the ponderomotive potential created by the electric field of a single-cycle THz pulse^{10–14} was demonstrated. In Ref. 10, it was shown that right after the excitation of n -GaAs by a THz pulse with peak electric field $E_{THz} \simeq 100$ kV/cm, the effective mass of electrons initially occupying the bottom of Γ valley ($m_\Gamma = 0.063m_0$) drastically increases and reaches the values of $m \simeq 0.3m_0$, more typical for the L and X valley states in GaAs ($m_L = 0.23m_0$, and $m_X = 0.43m_0$).^{27,28} Here m_0 is the electron rest mass. The THz saturable absorption based on this mechanism, shown in Fig. 1(a), was observed by us in various n -doped semiconductors.²⁹ The temporal response of THz nonlinearity of n -GaAs is near instantaneous, as shown in Fig. 1(b). This measurement is a result of THz pump-THz probe (TPTP) spectroscopy^{10,12–14} where our n -GaAs sample with the thickness $d = 0.4$ mm, $N = 5 \times 10^{15}$ cm⁻³, and $\tau_r = 94$ fs was excited by a THz pump pulse with peak $E_{THz} \simeq 200$ kV/cm. The near-instantaneous bleaching of the sample is followed by a slower recovery as the electrons return to the bottom of the Γ valley.³⁰ This and all other measurements in this work were performed at room temperature.

We studied the SPM of single-cycle THz pulses in our n -GaAs sample in a nonlinear THz TDS experiment set up in transmission configuration.²⁹ The frequency spectrum of the THz pulses, generated by optimized optical rectification

of 800 nm, 100-fs laser pulses in lithium niobate (LN),^{2–4} covered the range 0.1–3 THz, thus containing many octaves of frequencies. The peak electric field E_{THz} in the generated THz pulses was adjusted in the range of 9–292 kV/cm using a pair of wire-grid polarizers positioned after the THz emitter in the spectrometer.²⁹ THz transmission through the polarizers is nominally frequency independent. The THz pulses were recorded in the time domain using free-space electro-optic sampling.^{17,18}

As shown in Fig. 2, for each value of peak E_{THz} in the generated THz pulse, a reference (travelling through the optical path in the spectrometer in vacuum) and a sample (travelling through the same geometrical path, but with the sample inserted into it) THz pulses,^{17,18} centered around the time delays of 0 and 3.3 ps, respectively, were recorded. A clear THz saturable absorption (i.e., increase in THz transmission)²⁹ in our n -GaAs sample with growth in peak electric field E_{THz} is observed. In Figs. 2(a) and 2(c), the measured reference and sample THz pulses for the two extreme values of peak E_{THz} , 292 and 9 kV/cm, are shown as examples of raw data. Here and below, all mentioned peak values of E_{THz} correspond to that of the reference THz pulse and are reported as measured at the position of the sample.

In Fig. 2(b), a two-dimensional plot shows the reference and sample pulses normalized to their respective peak values, for the whole range of peak E_{THz} in our experiments. As apparent from this plot, the time delay between the reference and the sample THz pulses in n -GaAs increases with increasing peak E_{THz} , which is a direct signature of SPM. The dashed black line in Fig. 2(b) shows the estimated group delay (i.e., “delay as a whole”)²⁹ of a THz pulse in the material as a function of peak E_{THz} . In Figs. 2(d) and 2(e), the normalized reference and sample pulses for the two extreme values of peak E_{THz} of 9 and 292 kV/cm are shown. The difference between the two reference wave forms in Fig. 2(d) is fairly small: there is no observable time shift, and there is only a very small change in the pulse shapes, which is due to nonideality of the THz wire-grid polarizers used for adjustment of the peak THz field. The difference between the two sample wave forms in Fig. 2(e) is, however, quite noticeable. The sample wave form corresponding to a stronger E_{THz} clearly experiences a larger time delay as well as a certain reshaping. Figure 2 is therefore the direct time-domain observation of THz SPM occurring in a single-cycle regime. In Fig. 2(f), we show

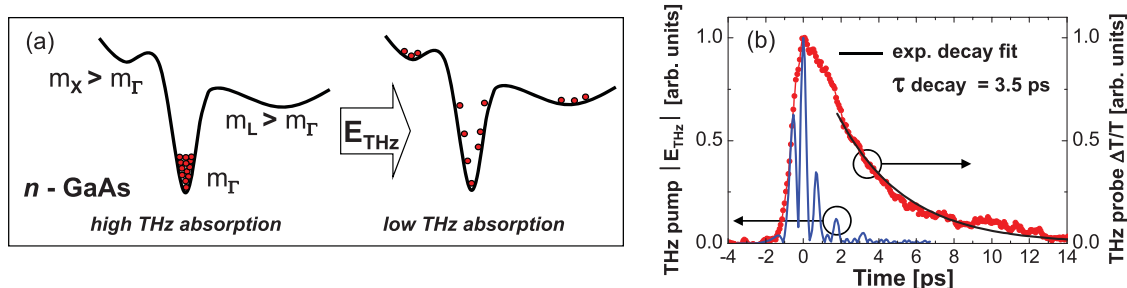


FIG. 1. (Color online) (a) Mechanism of THz nonlinearity in n -GaAs, based on carrier heating in the electric field of a THz pulse, leading to a decrease of plasma frequency ω_p and saturation of THz absorption. (b) Temporal dynamics of THz nonlinearity in n -GaAs, observed in a transmission-mode TPTP measurement. Near-instantaneous bleaching of the sample via carrier-heating in the THz field is followed by a slower recovery due to electron cooling.

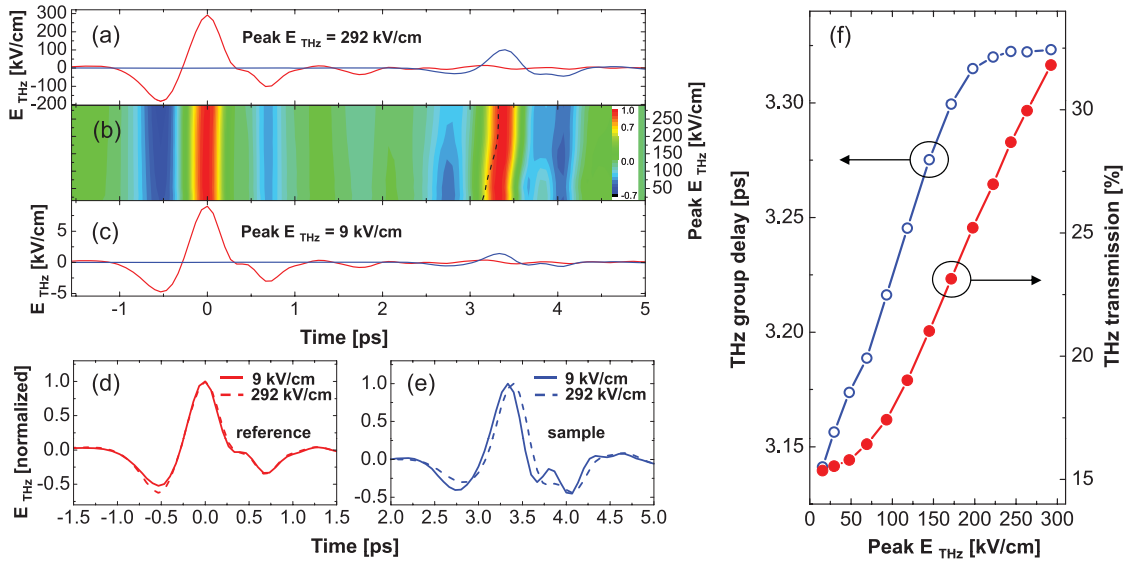


FIG. 2. (Color online) THz SPM in n -GaAs in the time domain. Peak E_{THz} of reference THz pulse in (a) is 292 kV/cm, and in (c) is 9 kV/cm. (b) Reference and sample pulses normalized to their maxima, for the whole range of peak E_{THz} of 9–292 kV/cm. Black dashed line: estimated group delay of the sample pulse. Normalized reference (d) and sample (e) pulses for the cases of peak E_{THz} of 9 and 292 kV/cm, demonstrating the SPM in the sample. (f) Amplitude frequency-integrated transmission coefficient, and estimated group delay of a sample pulse as a function of peak E_{THz} .

the connection between the saturable absorption and SPM in our sample by plotting both the THz frequency-integrated amplitude transmission coefficient and an estimated group delay of the sample pulse as a function of peak E_{THz} . The observed increase in the transmission coefficient is more than twofold, and the increase in the group delay exceeds 150 fs, making it a noticeable fraction of the duration of the THz cycle.

We now transfer to the frequency domain by using the Fourier transforms of the measured THz pulses from Fig. 2.^{17,18} In Fig. 3, we show the SPM as a nonlinear, THz-field dependent contribution to the refractive index of n -GaAs, calculated as a correction to the refractive index spectrum measured at the weakest peak E_{THz} , $\Delta n(\omega) = n(\omega, E_{\text{THz}}) - n(\omega, 9\text{kV/cm})$. A very strong, and also frequency-dependent, dynamics of $\Delta n(\omega)$ is observed with increase in peak E_{THz} from 9 to 292 kV/cm. In the inset, the examples of estimated³¹ absorption spectra are shown for the same range of peak E_{THz} . Interestingly, the refractive index nonlinearity is found to be both *negative* and *positive* within the bandwidth of the same single-cycle THz pulse, making it quite a unique situation in nonlinear optics (though quite understandable given the ultra-broadband nature of single-cycle pulses). These negative and positive trends in the dynamics of Δn at the frequencies below and above approximately 0.5 THz, with increase in peak E_{THz} , are shown with blue arrows in Fig. 3. The maximum refractive index changes in our measurements were as large as $\Delta n = -0.13$ to $+0.08$, in the spectral range 0.3–2.4 THz. This corresponds to the nonlinear phase delay $\Delta\tau_\phi = \Delta n d/c$ in the range of -173 to $+107$ fs, acquired by the THz signal at different frequencies in our 0.4-mm thick sample, as also shown in Fig. 3.

In our specific case, most of the spectrum of the THz pulse (shown as grey area in Fig. 3) was in the spectral range of positive index nonlinearity, which results in the increasing

group delay of the THz pulse at higher peak E_{THz} (see Fig. 2). However, if the THz pulse spectrum belonged to the range below 0.5 THz, the decrease in group delay with increase in E_{THz} would occur instead.

Inherent to SPM is spectral reshaping of the optical signal,^{36,37} which can lead to both spectral broadening and compression within the same NLO system (see, e.g., Ref. 32). In Fig. 4(a), it is illustrated by the dependency of the ratio of effective spectral bandwidths of the sample and reference pulses $\Delta\omega_{\text{sam}}/\Delta\omega_{\text{ref}}$ on peak E_{THz} .³³ If this ratio is

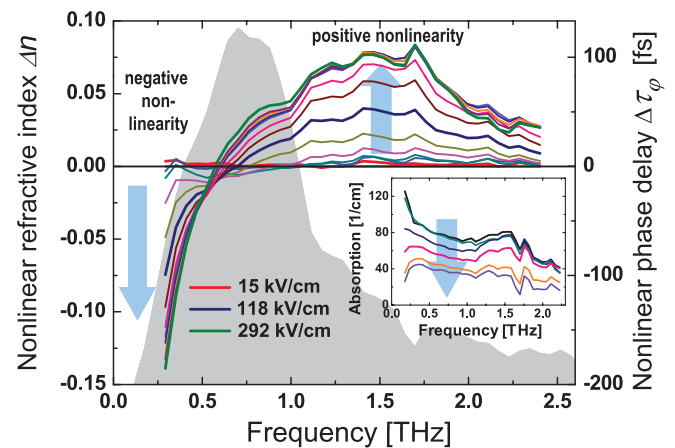


FIG. 3. (Color online) THz SPM in n -GaAs in spectral domain. Nonlinear contribution to refractive index Δn , and corresponding nonlinear phase delay as a function of frequency and peak E_{THz} in the range 9–292 kV/cm. The amplitude spectrum of reference THz pulse is shown as a background. Inset: selected estimated absorption spectra in the same range of peak E_{THz} . Blue arrows show the positive and negative refractive index nonlinearity, and decrease in absorption, with increasing peak E_{THz} .

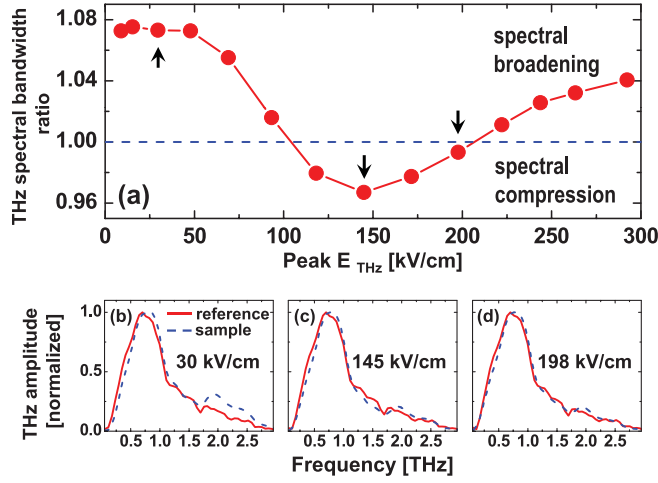


FIG. 4. (Color online) Nonlinear spectral broadening and compression of a THz pulse in n -GaAs. (a) The ratio of effective bandwidths of the sample and reference pulses, as a function of peak E_{THz} . (b)–(d) Examples of spectral dynamics: normalized amplitude spectra of reference and sample THz pulses measured at peak THz field values of 30, 145, and 198 kV/cm, indicated by arrows in (a).

greater (smaller) than unity, then relative spectral broadening (compression) of a THz pulse in a sample takes place. We observed a spectral compression and broadening of a THz pulse in our sample by approximately -3% to $+7\%$. In Figs. 4(b)–4(d), the normalized amplitude spectra of reference and sample THz pulses at selected values of peak E_{THz} are shown, exemplifying the spectral broadening, compression, and virtually no change, respectively, of THz pulses in n -GaAs.

In a *movie* (see Supplemental Material³⁸) we visualize the correlation between the THz pulse transmission, delay, and spectral dynamics as a function of peak E_{THz} , also showing the field-dependent evolution of THz pulse spectrograms³⁴.

In general, the nonlinear-optical spectral dynamics will depend on the combination of pulse chirp, index nonlinearity, and frequency-dependent nonlinear absorption.^{36,37} As the THz SPM finds its origin in the ponderomotive acceleration of free electrons, the THz pulse shape at each moment during its propagation becomes an important factor in precise time-domain modeling of THz nonlinearities in semiconductors, which can only be achieved using advanced numerical methods.^{6,14}

We note that the link between the refractive index and absorption (or gain) nonlinearities is fundamental, and is used, e.g., in semiconductor slow/fast light devices for the telecom range (see, e.g., Refs. 35 and 36). We also note that the reshaping of a THz signal generated in a LN crystal under variable optical pump strength was reported and assigned to THz SPM in Ref. 3, but later study clearly related this effect to the optical-range nonlinearity of the laser pump pulse in LN.³⁹ The reshaping by SPM of a THz pulse in InSb undergoing impact ionization was reported,⁸ however, without the spectral-domain analysis.

Now we illustrate the observed trends in nonlinear absorption and refractive index by simple modeling. In Fig. 5, the measured *linear* THz spectra of our sample are shown (symbols) along with the Drude fit using the parameters

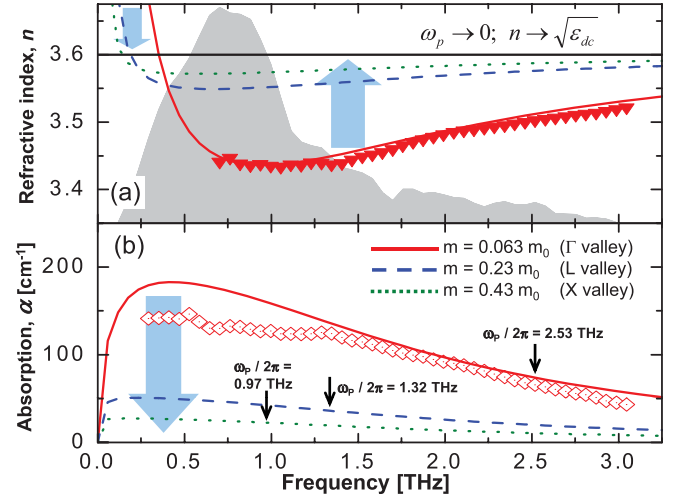


FIG. 5. (Color online) Blue arrows: trends in (a) refractive index and (b) absorption THz spectra of n -GaAs with decrease in ω_p . Spectra measured in linear regime (symbols) and calculated using a DS model with $N = 5 \times 10^{15} \text{ cm}^{-3}$, $\tau_r = 94 \text{ fs}$, and $c_{\text{DS}} = -0.15$ for the electron effective mass of Γ (red solid line), L (blue dashed line), and X (green dotted) valleys. Amplitude spectrum of a reference THz pulse is shown in the background of (a). Black arrows indicate the corresponding ω_p values. Horizontal line in (a) corresponds to $\omega_p = 0$, when $n = \sqrt{\epsilon_{\text{dc}}} = 3.6$.

N and τ_r described above, $n = \sqrt{\epsilon_{\text{dc}}} = 3.6$,⁴⁰ and $m = m_{\Gamma}$ (solid lines). For this fit, we used a Drude-Smith (DS) model incorporating the effective carrier localization into an ideal Drude model.^{24,25} The small localization parameter $c_{\text{DS}} = -0.15$ used here shows that our sample is very close to an ideal Drude plasma system described by Eq. (1). In the same figure, we show the calculated n and α spectra for the same sample parameters as before, but using the heavier effective masses $m = m_L$ and $m = m_X$ of the satellite valleys^{28,42} (dashed and dotted lines, respectively). Corresponding values for ω_p are shown in the figure using black arrows. It is clear that with decrease in ω_p the absorption decreases monotonously. The trend in refractive index with decreasing ω_p is the decrease from larger values at lower frequencies ($<0.5 \text{ THz}$) and increase from lower values at higher frequencies, approaching the background value of $n = \sqrt{\epsilon_{\text{dc}}}$ at $\omega_p = 0$. These trends in the dynamics of α and n , indicated by the blue arrows, exactly match the trends in observed saturable absorption and refractive index nonlinearity [see Figs. 2(f) and 3], including opposite signs of Δn at lower and higher frequencies. The large value of refractive index at lower frequencies in a metal or doped semiconductor directly follows from Eq. (1): it is known as Hagen-Rubens regime, and is characteristic for the frequency range $\omega \ll \tau_r^{-1}$.²³ The spectral position of zero index nonlinearity is thus defined by the electron momentum relaxation rate τ_r^{-1} , and can be theoretically predicted with reasonable accuracy, as shown by Figs. 3 and 5(a).

In conclusion, we have studied the SPM of a single-cycle THz pulse in a semiconductor, whose THz-range optical nonlinearity is based on the carrier heating in THz fields leading to the plasma frequency shift, and can be adequately

described by the Drude model. It can find its application in, e.g., THz-wave ultrahigh speed all-optical signal processing schemes, where THz SPM can be employed as successfully as in the optical domain,^{35–37} although the physical mechanisms of THz and optical range nonlinearities are very different.

Material engineering can be employed to minimize the effect of linear absorption on the propagation of THz pulses, as well as to control the electron momentum relaxation rate, which defines the sign of refractive index nonlinearity. Combination of smaller linear loss with engineered index nonlinearity will pave the way to further development of

THz nonlinear optics, and will enable THz supercontinuum generation and THz solitons in solid-state systems, which are presently only achievable in the optical range.

We are grateful to K. Yvind, J. Lægsgaard, J. Mørk (DTU Fotonik), and A. Cavalleri (University of Hamburg) for valuable discussions. We acknowledge the partial financial support from the Danish Proof of Concept Foundation (grant 7.7 Ultrahigh-speed wireless data communications), Danish Council for Independent Research - Technology and Production Sciences (FTP), and Max Planck Society.

*dmtu@fotonik.dtu.dk

¹P. A. Franken, A. E. Hill, C. W. Peters, and G. Weinreich, *Phys. Rev. Lett.* **7**, 118 (1961).

²K.-L. Yeh, M. C. Hoffmann, J. Hebling, and K. A. Nelson, *Appl. Phys. Lett.* **90**, 171121 (2007).

³J. Hebling, K.-L. Yeh, M. C. Hoffmann, and K. A. Nelson, *J. Sel. Top. Quant. Electron.* **14**, 345 (2008).

⁴M. C. Hoffmann and J. A. Fulop, *J. Phys. D* **44**, 083001 (2011).

⁵S. D. Ganichev and W. Prettl, *Intense Terahertz Excitation of Semiconductors* (Oxford University Press, Oxford, 2006).

⁶J. R. Danielson, Y.-S. Lee, J. P. Prineas, J. T. Steiner, M. Kira, and S. W. Koch, *Phys. Rev. Lett.* **99**, 237401 (2007).

⁷H. Hirori, M. Nagai, and K. Tanaka, *Phys. Rev. B* **81**, 081305 (2010).

⁸H. Wen, M. Wiczler, and A. M. Lindenberg, *Phys. Rev. B* **78**, 125203 (2008).

⁹M. C. Hoffmann, J. Hebling, H. Hwang, K.-L. Yeh, and K. Nelson, *Phys. Rev. B* **79**, 161201 (2009).

¹⁰M. C. Hoffmann, J. Hebling, H. Y. Hwang, K.-L. Yeh, and K. A. Nelson, *J. Opt. Soc. Am. B* **26**, A29 (2009).

¹¹F. H. Su *et al.*, *Opt. Express* **17**, 9620 (2009).

¹²J. Hebling, M. C. Hoffmann, H. Y. Hwang, K.-L. Yeh, and K. A. Nelson, *Phys. Rev. B* **81**, 035201 (2010).

¹³G. Sharma *et al.*, *IEEE Photonics J.* **2**, 578 (2010).

¹⁴F. Blanchard, D. Golde, F. H. Su, L. Razzari, G. Sharma, R. Morandotti, T. Ozaki, M. Reid, M. Kira, S. W. Koch, and F. A. Hegmann, *Phys. Rev. Lett.* **107**, 107401 (2011).

¹⁵M. C. Hoffmann, B. S. Monozon, D. A. Livshits, E. U. Rafailov, and D. Turchinovich, *Appl. Phys. Lett.* **97**, 231108 (2010).

¹⁶T. Ogawa, S. Watanabe, N. Minami, and R. Shimano, *Appl. Phys. Lett.* **97**, 041111 (2010).

¹⁷M. Tonouchi, *Nature Photon.* **1**, 97 (2007).

¹⁸P. U. Jepsen, D. G. Cooke, and M. Koch, *Laser Photonics Rev.* **5**, 124 (2011).

¹⁹T. Brabec and F. Krausz, *Phys. Rev. Lett.* **78**, 3282 (1997).

²⁰F. Shimizu, *Phys. Rev. Lett.* **19**, 1097 (1967).

²¹R. R. Alfano and S. L. Shapiro, *Phys. Rev. Lett.* **24**, 592 (1970).

²²R. Huber, F. Tauser, A. Brodschelm, M. Bichler, G. Abstreiter, and A. Leitenstorfer, *Nature (London)* **414**, 286 (2001).

²³M. Dressel and G. Grüner, *Electrodynamics of Solids: Optical Properties of Electrons in Matter* (Cambridge University Press, Cambridge, 2002).

²⁴N. V. Smith, *Phys. Rev. B* **64**, 155106 (2001).

²⁵H. Němec, P. Kužel, and V. Sundström, *Phys. Rev. B* **79**, 115309 (2009).

²⁶Here, we can ignore, for simplicity, the dispersion due to a phonon contribution to $\hat{\epsilon}$, which is generally independent of free carriers.

²⁷K. Brennan and K. Hess, *Solid-State Electron.* **27**, 347 (1984).

²⁸A static Gunn field of GaAs is about 5 kV/cm. A terahertz signal with the central frequency of 1 THz and with the peak $E_{\text{THz}} = 100$ kV/cm, applied to the Γ valley electron, has a ponderomotive energy of about 1.8 eV, clearly exceeding the Γ -L and Γ -X energy separations of 0.33 and 0.52 eV, respectively,²⁷ thus making intervalley transitions possible.

²⁹M. C. Hoffmann and D. Turchinovich, *Appl. Phys. Lett.* **96**, 151110 (2010).

³⁰N. A. van Dantzig and P. C. M. Planken, *Phys. Rev. B* **59**, 1586 (1999).

³¹The absorption spectra were calculated based on the Fresnel losses at the air-sample interfaces,¹⁸ corresponding to the background refractive index $n = \sqrt{\epsilon_{\text{dc}}}$. The influence of the nonlinear index contribution $\Delta n \ll \sqrt{\epsilon_{\text{dc}}}$ can be neglected in this case.

³²X. Liu, J. Lægsgaard, and D. Turchinovich, *Opt. Express* **18**, 15475 (2010).

³³ $\Delta\omega = \int_{\omega} E(\omega)d\omega/\max[E(\omega)]$, where $E(\omega)$ is Fourier amplitude of the corresponding terahertz pulse.

³⁴Q. Lin, J. Zheng, J. Dai, I.-C. Ho, and X.-C. Zhang, *Phys. Rev. A* **81**, 043821 (2010).

³⁵M. van der Poel, J. Mørk, and J. M. Hvam, *Opt. Express* **13**, 8032 (2005).

³⁶C. J. Chang-Hasnain and S.-L. Chuang, *J. Lightwave Technol.* **24**, 4642 (2006).

³⁷G. P. Agrawal, *Nonlinear Fiber Optics* (Academic Press, Amsterdam, 2007).

³⁸See Supplemental Material at <http://link.aps.org/supplemental/10.1103/PhysRevB.85.201304> for a movie, showing the evolution of THz pulses in time domain, and their spectrograms in time- and frequency domain, as the peak THz field changes.

³⁹M. Nagai, M. Jewariya, Y. Ichikawa, H. Ohtake, T. Sugiura, Y. Uehara, and K. Tanaka, *Opt. Express* **17**, 11543 (2009).

⁴⁰D. Grischkowsky, S. Keiding, M. van Exter, and Ch. Fattinger, *J. Opt. Soc. Am. B* **7**, 2006 (1990).

⁴¹J. Pozela and A. Reklaitis, *Solid-State Electron.* **23**, 927 (1980).

⁴²The momentum relaxation rate in GaAs at $N \leq 10^{17}$ cm⁻³ is shown to have a negligible dependency on the driving electric field,⁴¹ therefore the value of $\tau_r = 94$ fs, obtained by linear terahertz spectroscopy, was used throughout this model.